International Journal of Thermal Sciences 189 (2023) 108282

Contents lists available at ScienceDirect

International Journal of Thermal Sciences

journal homepage: www.elsevier.com/locate/ijts

Thermal conduction in karst terrains dominating cave atmosphere temperatures: Quantification of thermal diffusivity

David Domínguez-Villar [a,*], Kristina Krklec [b], Francisco J. Sierro [a]

[a] Department of Geology, Faculty of Science, Universidad de Salamanca, Plaza de Los Caídos s/n, 37008, Salamanca, Spain
[b] Department of Soil Science, Faculty of Agriculture, University of Zagreb, Svetošimunska 25, 10000, Zagreb, Croatia

ARTICLE INFO

Keywords:
Temperature
Thermal conduction
Thermal diffusivity
Cave
Karst

ABSTRACT

The relatively stable temperature of most cave interiors is caused by the transfer of the surface atmosphere temperature signal to the karst underground by thermal conduction. Transferring underground thermal signals by conduction implies the amplitude attenuation of the external thermal anomaly as well as a signal delay. The magnitude of these attenuation and delay effects is proportional to the thickness of bedrock cover above the cave and is controlled by the bedrock thermal diffusivity. Here we present 5-year temperature record of Los Pilones Cave, in central Spain, where advection has a limited control on thermal anomalies all year round. Thus, thermal conduction dominates the thermal variability in the cave, with simulations of a 1-D thermal conduction model explaining up to 94% of the variability observed. Thermal attenuation and signal delays are highly correlated with the thickness of bedrock cover ($r^2 = 0.95$ in both cases), enabling the calculation of a thermal diffusivity of $5.07*10^{-7} \pm 1.27*10^{-7}$ m^2/s. The calculated thermal diffusivity is in the range of available values measured in laboratory for carbonate lithologies, although differs beyond uncertainty from the limited number of studies that calculated this value from field observations in karst. Thus, local rock properties significantly impact thermal diffusivities, and more experimental studies are required to show a complete distribution of this value in karst settings. The reported uncertainty, that was calculated using different time windows within the studied period, represents a variability of 23% on the thermal diffusivity. Karst terrains are mostly composed of three phases, rock, air and water, that have different thermal properties. Thus, variability of the water content in the rock porosity through time is likely a significant control on the measured uncertainty. Since temperature in the studied cave has a minor component affected by advection, this cave represents a paradigmatic location to observe the important role of thermal conduction in caves. Therefore, conclusions from this study can be useful to better understand thermal regimes and interannual trends of most cave interiors despite occurrence of variable impacts of seasonal ventilation dynamics in cave temperature records. In addition, the mechanism of thermal conduction results in a thermal decoupling between the surface and cave atmospheres affecting cave microclimate, which has important implications for multiple disciplines interested in karst underground environments.

1. Introduction

The interior of the Earth provides heat to the crust, where the heat flux depends on the geological characteristics of the region that affect geothermal gradients [1]. Thus, at depths of several hundred meters, the temperature of the crust increases with depth following the regional or even local geothermal gradient (e.g. Ref. [2]). However, the energy flux received from the Sun is c. 4000 times larger than the energy flux of the Earth's interior [3]. So, in the upper section of the crust (typically several hundred meters) the underground temperature is dominated by the temperature of the atmosphere, an impact that decreases with depth but that can reach depths >500 m (e.g. Ref. [4]). The impact of the atmosphere on the underground temperature is more obvious in the top tens of meters, where seasonal atmospheric variations produce seasonality of the underground temperature [5]. The mechanisms for temperature transfer from the atmosphere to the underground are dominated by heat conduction [6,7]. When atmosphere temperature signal is transferred underground by conduction, the anomalies are attenuated with depth and the signal records certain delay that increases with depth [8]. Daily temperature cycles are typically attenuated within

* Corresponding author.
E-mail address: ddvillar@usal.es (D. Domínguez-Villar).

https://doi.org/10.1016/j.ijthermalsci.2023.108282
Received 19 January 2023; Received in revised form 4 March 2023; Accepted 9 March 2023

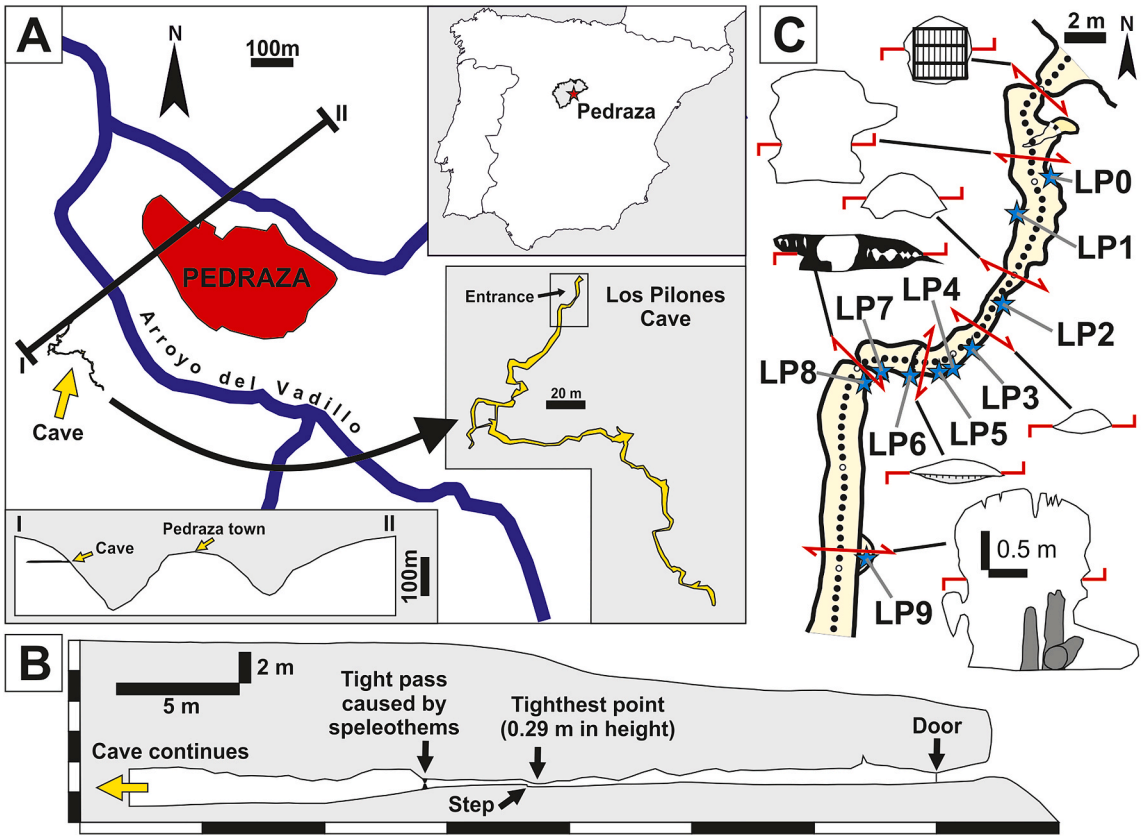

Fig. 1. Setting of Los Pilones Cave. A) Location and topography of Los Pilones Cave in the surroundings of Pedraza town. Upper right inset graph shows the location of Pedraza town within the Iberian Peninsula, the lower right inset graph shows Los Pilones Cave topography, and the lower left inset graph shows the topographic profile across Arroyo del Vadillo valley from points I to II. B) Longitudinal profile of the entrance corridor of Los Pilones Cave. C) Topographic map of Los Pilones Cave including multiple cross sections to illustrate the cave morphology. Blue stars show the location of the sites (LP0 to LP9) where temperature was measured inside the cave. Black dots along the center of the corridor indicate the sites, half meter apart, where height of the ceiling was measured.

2 m, thermal anomalies of seasonal cycles are muted below depths of c. 20 m, whereas decadal to millennial cycles can be recorded tens to hundreds of meters underground [9,10]. The thermal diffusivity (κ), also known as thermal diffusion coefficient, is the parameter that modulates the attenuation and delay of thermal signals through a medium and, as other thermal properties, depends on the composition of the medium [11].

Most caves are developed in karst terrains which are regions composed of soluble rocks [12]. Caves in karst are underground environments which temperature typically has a limited thermal variability in relation to the surface atmosphere temperature (SAT) above the cave. The cave atmosphere temperature (CAT) in the interiors of most caverns is stable and approximates to the mean annual SAT above the cave [13–15]. Since the heat contained in a certain volume of carbonate rock is c. 1800 times larger than the heat contained in the same air volume [16], for most caves, their temperature is controlled by the cave walls [17]. In karst terrains, as in terrains formed by different lithologies, conduction dominates the heat transfer from the external atmosphere to the underground [15,18], which explains the link of SAT and CAT [13,19]. However, due to the soluble nature of karst, caves and conduits form networks where water and air flow, facilitating the advection of heat. Advection of water in the phreatic zone of karst limits the impact of geothermal gradients in caves developed in the vadose zone of karst [5,20]. However, temperature in the vadose zone of karst increases with depth, typically 0.2–0.4 °C/100 m, due to the adiabatic gradient in the atmosphere and the transformation of the potential energy of recharged water to heat [21–23]. The moisture in the underground atmosphere also plays a certain role in the underground temperature due to latent heat [24], which is responsible of the variability in cave adiabatic gradients.

The role of advection of air in the vadose zone of karst is more obvious near cave entrances, where air flow is more dynamic (e.g. Refs. [25,26]). In cave interiors, far from their entrances, air advection can also result in perturbations of CAT signals. Air advection in caves is caused by air density and/or barometric gradients [27], which commonly results in seasonal ventilation dynamics (e.g. Ref. [28]). During the season of enhanced cave ventilation, the CAT signal usually records high-frequency oscillations related to variations in air flow and the external temperature. These fluctuations occur almost synchronously (i.e., <1 day) within the cave system and are independent to cave depth [29,30]. On the other hand, during the season of wanned cave ventilation, advection typically has limited to no impact on the CAT signal that records low-frequency oscillations resulting from the thermal signal being transferred by conduction to the cave. Evaporative conditions in cave atmospheres can also affect CAT signals due to the impact of latent heat (e.g. Ref. [31]). Despite advection and latent heat introduce thermal variability at seasonal and/or event timescales [9,32], the supra-seasonal CAT variability in most caves is still dominated by thermal conduction [33].

Cave temperature is a key component in studies on cave microclimate, cave art conservation, underground ecology and paleoclimate reconstructions. Although the role of thermal conduction to transfer temperature anomalies to the caves is well known [18,34–36], most scientists working in cave environments ignore the importance that the depth at which caves are located has on the cave microclimate dynamics and its record in speleothems. Here we present a study focused on the transfer of SAT signal to the cave entrance of Los Pilones Cave in central Spain. Thermal conduction dominates the CAT signal even in the

entrance of the cave due to the narrow passage of the entrance that limits the thermal impact of advection. The aim of our research is to provide a robust calculation of the thermal diffusivity in the studied cave and to highlight the impact that thermal conduction has on the transfer of SAT signals to caves or underground environments. Since there is a very limited number of studies that experimentally calculated thermal diffusivities in natural karst environments [35,36], this research represents a significant advance in the field. Comparison of thermal models and observations in a system with limited interferences also provides the opportunity to study in detail the specific properties of thermal conduction in karst terrains, where the medium is not uniform in space and time due to the heterogeneous distribution of porosity and the variable proportion of water flowing through that porosity during different periods. In addition, showing unequivocally how a common SAT signal provides diverse CAT records that depend on specific site characteristics within the cave, could benefit other scientists to understand the key role of thermal conduction controlling temperature in caves or other underground environments.

2. Materials and methods

2.1. Study site

Los Pilones Cave is located in the province of Segovia, central Spain (41°07′49″N 3°49′03″W). The same cave is also referred by the name of Cueva Nueva in early topographic maps [37]. Los Pilones Cave is developed in the slope of the valley of Arroyo del Vadillo, in front of the town of Pedraza, and the entrance to the cavity is located at 1069 m above sea level. The cave is a sub-horizontal gallery several hundred meters in length with frequent narrow passages, absence of large halls and a single entrance. The valley is dissecting a plateau that represents a degraded erosive pediment. The cave is c. 20–30 m below the plateau and c. 80 m from the bottom of the valley. Los Pilones Cave is developed in Cretaceous dolomites and biocalcarenites with dolomitic cement deposited in shallow marine environments [38]. The dolomite beds often have cross stratification (biocalcarenite bars up to 1 m thick) and bioturbation is common at the top of some sequences, although recrystallization (i.e., dolomitization) often prevents identification of detailed sedimentary structures or the original sediment components. The series is gently dipping towards the South.

The cave entrance is at the base of a 6 m cliff where a nearly circular opening (<1 m in diameter) gives access to the cavity (Fig. 1). A metal door is installed at the entrance that allows natural ventilation of the cave. The ground is composed of a detrital sediment with gentle slopes although disturbance of the original stratigraphy has resulted in occasional steps on the ground. The ceiling of the cave entrance has an irregular morphology with cupulas and different narrow sections that often are <0.5 m in height. The gallery has its lowest height (0.29 m) at 18 m from the entrance in a curve that changes the orientation of the conduit. A step elevates the ground 0.1 m right after this tight point of the gallery (when entering the cave) which represents a significant topographic barrier. Following a fissure in the ceiling, a set of speleothem columns, stalactites and stalagmites cross the narrow gallery forcing an additional bottle neck that gives entrance to a more ample passage in the cave 22 m from the entrance. Ventilation of the cave does not result in air currents that could be felt, but spot measurements of CO_2 during different seasons confirms that the cave is well ventilated all year round (i.e., CO_2 concentrations oscillate between 800 and 1500 ppmv).

The climate in the region of Pedraza is warm-summer Mediterranean (Csb) according to Köppen classification [39]. The average annual temperature is 10.5 ± 0.5 °C estimated from regional measurements during the 30-year period from 1981 to 2010, whereas the average annual precipitation during the same period was 550 ± 50 mm [40]. The plateau is covered by a patchy forest dominated by evergreen oaks and limited shrubs, since the area is occasionally used as pastures for cattle. Rock outcrops are common in the slope of the valley, often resulting in small cliffs with limited lateral continuity. Soil is patchy, depending on the local topography, although profiles up to 0.5 m occur favored by accumulations of gravitational material creating poorly evolved regosols.

2.2. Cave topography

Topographic measurements of the cave and the surface on top of the cave were performed using a DISTO x2 laser equipped with a digital compass [41] supported by a target to define topographic stations. All topographic data were measured in relation to a station of origin, located on the ground at the entrance of the cave. Measurements were performed twice in both directions between stations, reverse measurements were recalculated for direction and the average of the four measurements was averaged to position every single station. Measurements with outlier values were repeated before being averaged. Stations were designed to be capable to close polygons enabling to evaluate topographic uncertainties. Data were processed with the software Visual Topo 5.11 [42] that redistributes uncertainties through the measurements minimizing punctual errors. In the entrance sector of the cave, 28 stations were positioned. Since the ceiling of the cave is more irregular than the ground, a detailed profile was conducted to calculate accurately the thickness of rock above the cave. Thus, every 0.5 m along center of the gallery, vertical measurements were obtained through a 35 m profile along the entrance corridor. Coordinates (X and Y) were obtained graphically, whereas ground elevation was interpolated from data between topographic stations which allowed the calculation of the elevation of the ceiling of the cave in relation to the station of origin. A total of 154 stations were measured on the surface over the cave entrance to create a high-density network of points referenced to the station of origin. The detailed surface topography was interpolated and projected above the cave. We extracted the elevation of the interpolated surface above the same coordinates of the center of the gallery and by subtracting the height of the ceiling, obtained the thickness of bedrock above the cave. The uncertainty of the measured thickness of bedrock cover above the cave, calculated as the 95% confident interval of the standard error of the mean of the stations that closed polygons (n = 11), is ±0.077 m.

2.3. Temperature measurements

Temperature was measured using loggers from Tinytag (i.e., TG-4100, TG-4500 and TGP-4017) that use 10 K NTC thermistors providing a precision of 0.5 °C, a nominal resolution of 0.001 °C and an actual resolution (i.e., above instrumental noise) that is 0.006 °C or better, as supported by replicated thermal responses to environmental changes [32](. To quantify the thermal variability among loggers, a specific calibration of the devices was conducted placing the loggers in an isothermal container within an environment with limited thermal oscillations. The reproducibility of the results was ±0.021 °C, calculated as the 95% confident interval of the standard error of the mean of tested loggers. Thermometers in the cave were placed directly over the ground or in ledges or small cavities within the walls. Most of the loggers were placed in the entrance corridor (n = 8), with spacings ranging from 0.5 m (in the tightest sections, to 5 m in the more ample sections. Two additional loggers were deployed in the inner section of the cave (i.e., beyond the speleothem columns that constrain the entrance corridor and that give access to a more ample gallery of the cave). One of them was deployed just beyond the speleothem columns, whereas the second logger was set in the ample section of this gallery. The thermometer outside the cave, located on top of the cave entrance corridor, was housed in a Stevenson screen mounted on a mast 2 m above the ground. Most of the loggers measured temperature during a 5-year monitoring period (i.e., 2017–2021), whereas two of the loggers (i.e., LP0 and LP1) started their record one year later. All loggers were set to record data at 30-min resolution and data was digested to calculate daily temperatures.

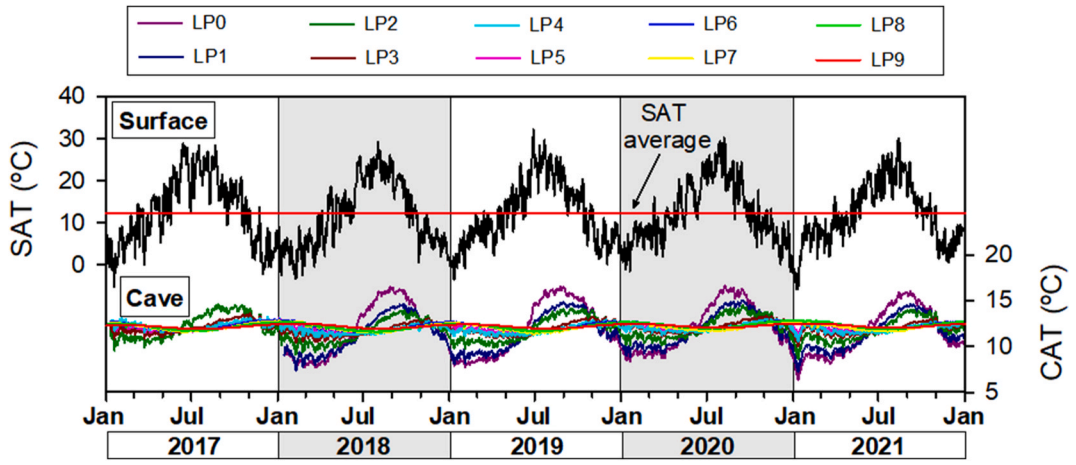

Fig. 2. Surface atmosphere temperature (SAT) measured above the cave and cave atmosphere temperature (CAT) measured in sites LP0 to LP9. Notice that thermal amplitudes of the different sites decrease with bedrock cover.

Small signal drifts were identified in two of the loggers (LP8 and LP9) accounting for accumulated drifts of 0.372 and 0.071 °C respectively. The drifts were identified by slight unusual long-term trends compared to nearby loggers and by sudden drops of temperature in the otherwise smooth and predictable thermal signals of the cave loggers. This sudden drop of temperature (i.e., 0.372 and 0.071 °C) occurred when all devices were opened to change their batteries during August 2021. Thermal drifts were likely caused by moisture entering through time into these two devices, affecting the resistance of their thermistors. Once these loggers were opened and initial moisture conditions reestablished, their signal registered the sudden drop of temperature making their readings compatible again with other thermometers. Signal drifts were corrected using square root equations (i.e., $y = a*x^2+b$) applied since the onset of the logger to the moment when the thermal drop was identified. Drift correction does not impact the results of this research that focuses on phase shift and seasonal thermal amplitude of the signals.

2.4. Data processing and thermal modelling

Daily temperature signals from all loggers were used for calculations. Phase shifts were calculated by performing cross correlation analysis on the 5-year period of the external thermal signal with the thermal signal from every cave logger. Thermal amplitude was calculated using two methods. Both methods use an arbitrary period of 11 days from which the day and temperature of every seasonal maximum and minimum were identified. Maximum and minimum thermal values of the external signal were calculated fitting a seasonal sinusoidal signal to measured values, resulting in extreme values recorded on 25th of January and 26th of July. The 11-day periods were centered in those two dates displaced by the phase shifts calculated during cross correlation analyses for each cave site where thermometers were installed. The extra day of the leap year was also accounted. The 11-day period was short enough not to bias from the expected maximum and minimum seasonal temperatures and to have duration enough to limit the impact of interannual variability of the phase shift and the local impacts of advection. The first method to calculate the thermal amplitude considers the average temperature during each 11-day period, whereas the second method considers the maximum value during each 11-day period to minimize the impact of advection events that tends to introduce cooler air into the cave entrance corridor. Since the second method provides better correlation coefficients between thickness of bedrock cover and thermal amplitudes, it was used in further calculations. Seasonal amplitudes are calculated as absolute values in the difference between consecutive maximum and minimum temperatures divided by two. The thermal amplitude of each cave thermal signal resulted in the average of all seasonal thermal amplitudes (up to 9 values for each location).

Thermal diffusivity (κ) can be calculated from the relationships between thickness of bedrock cover and phase shift or thickness of bedrock cover and natural logarithm of thermal anomalies [43] following

$$\kappa = \frac{\pi}{P \cdot k^2} \quad \text{[Eq. 1]}$$

where κ is expressed as m^2/s, P is the period expressed in seconds and k is the wave vector expressed in rad/m. This classical method to calculate thermal diffusivity is also known as Ångström method (e.g. Ref. [44]). The wave vector is calculated from the slope of the phase shift versus depth or the natural logarithm of the thermal amplitude versus depth. Since caves can have substantial differences in depth between ground and ceiling elevations, it is more precise to report the value of z as thickness of bedrock cover over the cave, which is expressed in meters. Since two independent methods can be used to calculate the wave vector and the thermal diffusivity (i.e., using phase shift or thermal amplitude), we use the average of wave vector obtained by both methods to calculate the thermal diffusivity in agreement with Smerdon et al. [43].

The uncertainty of the thermal diffusivity was calculated using an empirical approach to account for seasonal variability through the years. Seasonal sinusoidal signals for each depth were simulated according to

$$T_z = \overline{T}_z + A_z \cdot \sin\left(\frac{2 \cdot \pi \cdot t}{P}\right) - \varphi_z + \varepsilon \quad \text{[Eq. 2]}$$

where T_z is the sinusoidal thermal signal being modelled for each depth (z) measured in °C, $\overline{T}_z$ is the average temperature of the modelled signal in °C, A_z is the amplitude of the modelled signal at depth z reported in °C, t is time expressed in days and P is the period expressed in days (i.e., 365.25 d). The depth parameter (z) represents in fact the thickness of the bedrock cover, where the reference point ($z = 0$) is the ground level above each selected site in the cave. Bedrock thickness covers are calculated from a common reference point (the measurement station at the cave entrance), resulting in z values being relative depths in relation to the ground level. Thus, z values are independent of the elevation changes in the ground level along the slope of the valley. The parameter φ_z is the phase shift of each signal due to the delay time of the thermal signal being transferred by conduction to each depth, which is expressed in radians. Finally, ε is the initial phase shift of the cycle expressed in radians that allows fitting the simulated sinusoidal cycle to the external temperature signal. Parameters $\overline{T}_z$, A_z and φ_z were calculated from observational data during the 5-year period. Differences between simulated and observed cave records enabled calculating the variability of A_z and φ_z for each season (i.e., 6 months) in relation to those calculated using the full 5-year period. Thus, during the studied period, 10

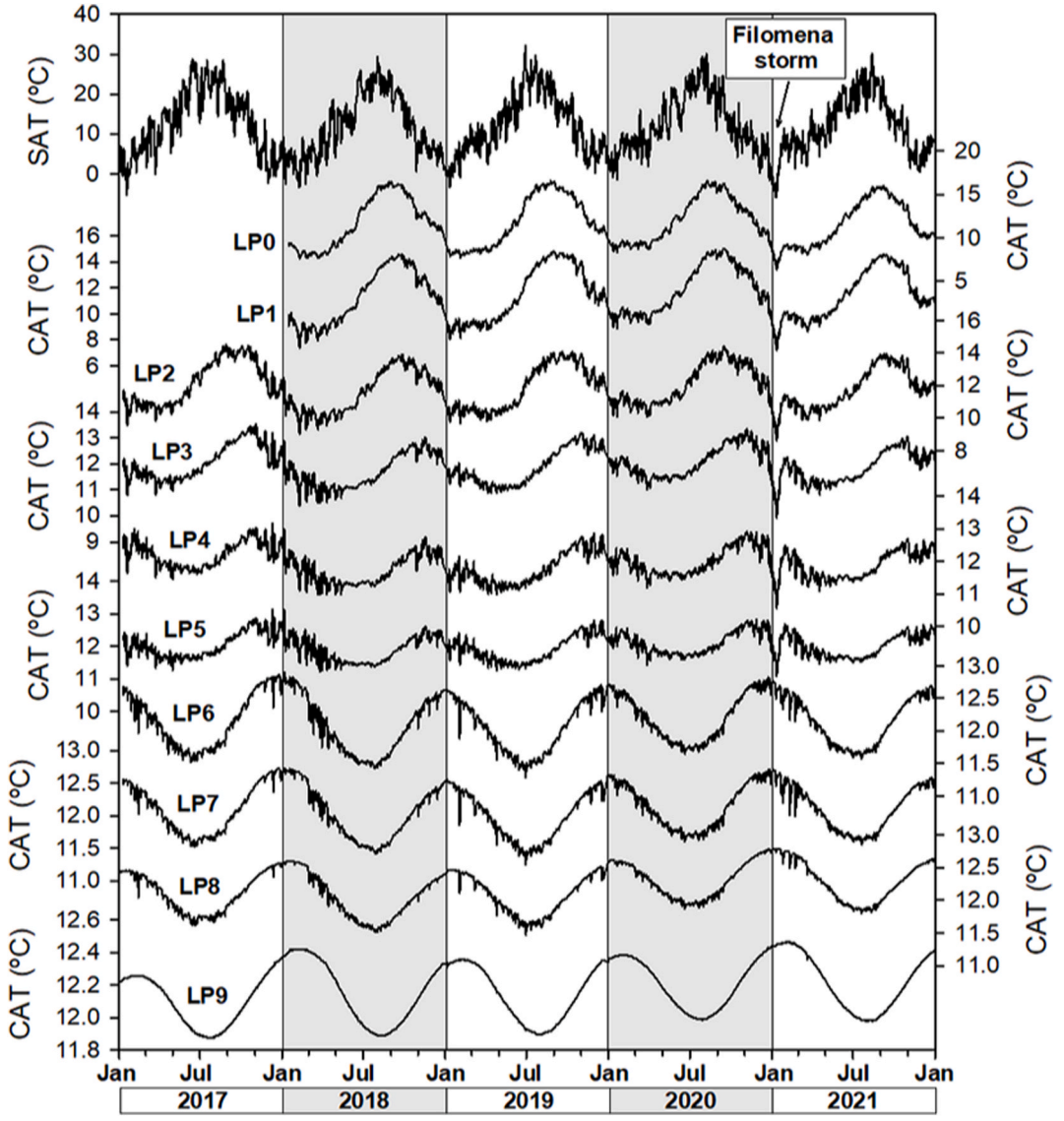

Fig. 3. Surface atmosphere temperature (SAT) measured above the cave and cave atmosphere temperature (CAT) measured in sites LP0 to LP9. Notice that each cave temperature record is shown with a different scale to better visualize the seasonality along different sites. The transfer of SAT signal underground by thermal conduction results in a progressive delay with thicker bedrock cover until accumulating 6 months of delay at site LP9. Temperature anomalies transferred to the cave by advection, such in the case of Filomena storm, are synchronous considering a 1-day resolution.

seasons were used to calculate standard deviations (SD) of A_z and φ_z. Considering a normal distribution and averages equal to A_z and φ_z during the 5-year period, the SD values were used to compute 100 Monte Carlo simulations for both parameters. These Monte Carlo simulations served to compute 100 wave vectors and thermal diffusivities which were used to calculate their 2 SD to constrain their variability. Since wave vector and thermal diffusivity can be calculated by two methods (i.e., thermal amplitude and phase shift), the uncertainty of the thermal diffusivity here provided is reported as the square root of the sum of the squares of the 2 SD of κ calculated by both methods.

3. Results

3.1. Calculation of the thermal diffusivity

The SAT recorded above the cave during the 5-year period had an average value of 12.27 °C (Fig. 2). On the other hand, records of CAT had a narrow range in their thermal averages (i.e., 11.50–12.17 °C), with cooler averages recorded in sites located closer to the cave entrance. These slight differences are mostly related to the effect of advection events causing temporary drops in cave temperature, which are attenuated in sections that are farther from the entrance. Thus, CAT at the site in the ample gallery beyond the entrance corridor, where impact of advection in the thermal variability is negligible, recorded 12.17 °C, very close to the average SAT.

Daily SAT and CAT varied seasonally. The amplitude of SAT was 9.61 °C, whereas the amplitude of CAT varied in loggers from 3.72 °C in the site located closer to the entrance to 0.23 °C in the site already located in the gallery beyond the speleothem columns constraint. The thermal attenuation of the seasonal thermal amplitude is progressive along the studied sites (Fig. 2), although the control of the attenuation is not the distance from the entrance but the thickness of bedrock cover above the cave, that in the case of the studied section of the cave gets progressively thicker overburden when distancing from the entrance increases (Fig. 1). In addition, the timing of maximum and minimum CAT varied along the studied sites (Fig. 3). Because the studied sites are located very close to each other, a progressive shift in the seasonal wave train is perfectly recorded. The progressive shift in the seasonal

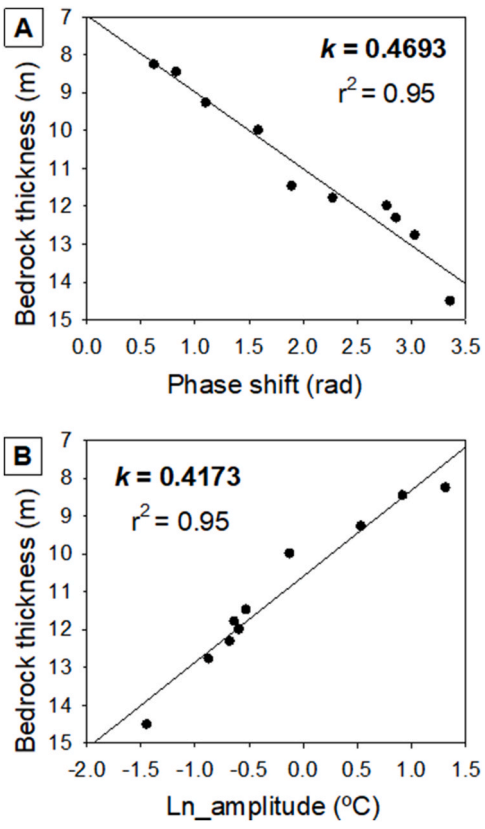

Fig. 4. Graphs showing the phase shift and the thermal amplitude in relation to the thickness of bedrock cover. The slope of these graphs is the wave vector (*k*) that is used to calculate the thermal diffusivity for this location.

amplitude of thermal signals shows that for an overburden of 14.5 m (site LP9), the phase shift has reached more than 6 months (i.e., 195 days) in relation to the SAT signal. Both, the thermal attenuation with depth and the phase shift of the thermal seasonality are strong arguments supporting thermal conduction being the dominant process controlling temperature in the cave entrance of Los Pilones Cave. Since the cave atmosphere receives heat from the walls, and galleries are sometimes >2 m in height, establishing the bedrock thickness above the cave is not straight forward even if precise topographic data is available. Therefore, two scenarios were considered to determine the exact bedrock thickness above each studied site. The first scenario considers the average elevation of the gallery to take into consideration that heat will be provided not just by the ceiling but also by the cave walls, which is particularly important when the gallery has high ceilings. The second scenario takes into consideration the height of the ceiling to calculate the bedrock thickness above the cave. Despite the limited dimensions of the entrance corridor, differences between these two scenarios account for z values that are up to 1.73 m in locations with higher ceilings. Thermal attenuation and phase shift with bedrock thickness above the cave show significant correlations for both scenarios. However, when mid-gallery elevations are used to calculate bedrock thickness, the Pearson's correlations with phase shift show determination coefficients (r^2) of 0.85, while the natural logarithm of the thermal amplitude results in determination coefficients (r^2) of 0.80 (p-values are <0.001 in both cases). On the other hand, when the ceiling elevation is used to calculate bedrock thickness both relationships show a stronger determination coefficient (r^2 = 0.95; p-value <0.01). Therefore, we use the bedrock cover calculated from the ceiling elevation to calculate wave vectors. Wave vectors resulted to be 0.4693 rad/m using the phase shift method, and 0.4173 rad/m using the thermal amplitude method. We calculate thermal diffusivity from the average of wave vectors (i.e., 0.4433 rad/m) resulting in $\kappa = 5.07*10^{-7}$ m^2/s. The uncertainty of thermal diffusivity was calculated using the distributions of seasonal phase shifts and thermal amplitudes instead of the 5-year period, enabling to conduct 100 Monte Carlo simulations to calculate the 2 SD of the 100 simulated thermal diffusivities. The squared root of the sum of the squares of the 2 SD thermal diffusivities obtained from the two methods used to calculate thermal diffusivity (i.e., phase shift and thermal amplitude) resulted in an uncertainty of $1.27*10^{-7}$ m^2/s. Therefore, the thermal diffusivity of the cave entrance of Los Pilones Cave during the 5-year period was $5.07*10^{-7}$ $\pm 1.27*10^{-7}$ m^2/s. A summary of the thermal diffusivity results, including the uncertainty calculations, is reported in Table 1. Considering the reported thermal diffusivity and using equation (2), CAT can be simulated using the bedrock cover of studied locations in the cave (Fig. 5). Determination coefficients (r^2) of the Pearson's correlation between observed CAT and simulated CAT provides values ranging from 0.58 to 0.94 (p-values <0.01). The fit of CAT simulations to the CAT observations is reported in Table 2. The CAT simulations using a 1-D thermal conduction model explains up to 94% of the variability of observed CAT. On average, the model explains >80% of the cave temperature variability, and even in the worst case (site LP4), the simulation explains >50% of the variability. Thus, we can confirm, that even in the entrance sector of Los Pilones Cave, CAT variability is dominated by thermal conduction and that 1-D thermal conduction simulations reproduce the most significant structure of measured temperature records (see Fig. 4).

3.2. Advection in the cave entrance

Sinusoidal equations simulated for each studied site using $\overline{T}_z$, A_z and φ_z during the full 5-year period reproduce the main thermal variability of CAT at each site (Fig. 5). Since no clear interannual trend or cycles were recorded in the 5-year period above the cave, periods beyond the annual cycle have limited impact on thermal conduction during the studied period. However, advection events were recorded and have a

Table 1
Summary table of wave vector (*k*) and thermal diffusivity (κ) calculations. Seasonal periods were used exclusively for the calculation of uncertainties, whereas the full 5-year period was used for the calculation of *k* and κ parameters. Bold numbers indicate final results.

Reference period for calculations	Method used for calculations	Wave vector (*k*) [rad/m]	Uncertainty [rad/m]		Thermal diffusivity (κ) [m^2/s]	Uncertainty [m^2/s]	
			2 SD[a]	SRSS[b]		2 SD[a]	SRSS[b]
Seasonal periods	Phase shift [c]	0.4707	±0.0355		$4.6261^{a}10^{-7}$	$\pm 0.7013^{a}10^{-7}$	
	Thermal amplitude[c]	0.4192	±0.0197		$5.7024^{a}10^{-7}$	$\pm 1.0538^{a}10^{-7}$	
	Average of methods	0.4449		**±0.0406**	$5.1642^{a}10^{-7}$		$\mathbf{\pm 1.2658^{a}10^{-7}}$
Full 5-year period	Phase shift	0.4693			$4.5199^{a}10^{-7}$		
	Thermal amplitude	0.4173			$5.7166^{a}10^{-7}$		
	Average of methods	**0.4433**		**±0.0406**	$\mathbf{5.0657^{a}10^{-7}}$		$\mathbf{\pm 1.2658^{a}10^{-7}}$

[a] 2 SD: 2 standard deviations.
[b] SRSS: Square root of sum of squares of 2 SD of phase shift and thermal amplitude methods.
[c] Phase shift and thermal amplitude *k* and κ values are the average of 100 Monte Carlo simulations based on average and SD of the 10 seasonal periods during the full studied period.

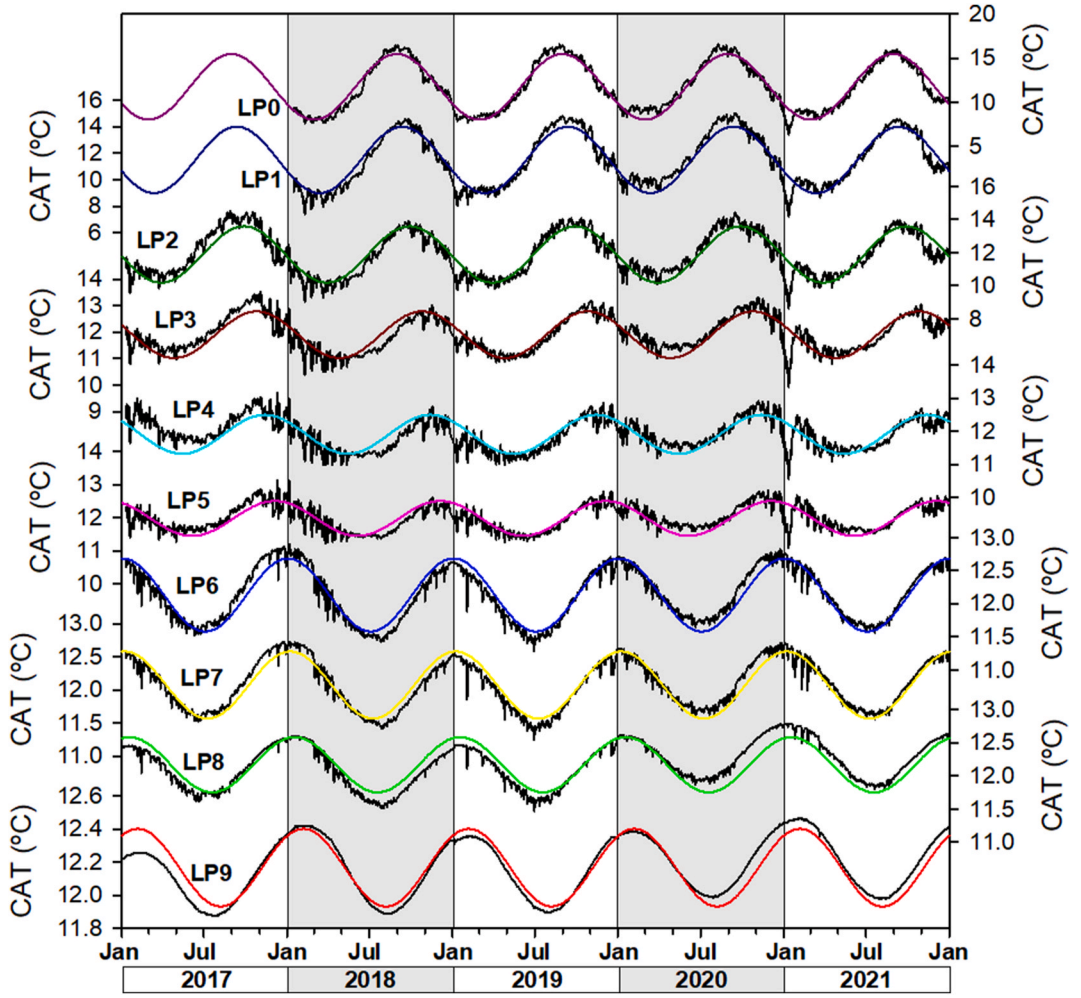

Fig. 5. Comparison of observed cave atmosphere temperature (CAT) with simulated CAT using a 1-D thermal conduction model. Notice that the temperature scales differ among cave sites to better visualize the seasonality along different sites.

Table 2
Determination coefficients between observed and simulated temperature records and various parameters of thermal variability in the simulated and the residual[a] series that impact the determination coefficients.

Site	Determination coefficient (r^2)	Simulated thermal amplitude (A_z) [°C]	Standard deviation of residuals (SD_{res}) [°C]	Ratio Ln $(A_z)/SD_{res}$
LP0	0.944	3.717	0.471	2.789
LP1	0.913	2.504	0.431	2.131
LP2	0.840	1.703	0.384	1.385
LP3	0.740	0.881	0.248	−0.510
LP4	0.582	0.588	0.212	−2.501
LP5	0.677	0.527	0.171	−3.752
LP6	0.908	0.552	0.067	−8.899
LP7	0.912	0.507	0.060	−11.413
LP8	0.822	0.417	0.039	−22.578
LP9	0.883	0.235	0.007	−198.047

[a] Residual series are the difference between the observed and simulated records after passed by a 1-year gaussian filter.

clear impact on most of the CAT sites along the entrance corridor. To obtain a record capturing the thermal impact of advection, observed CAT and simulated seasonal thermal signals (Fig. 5) were subtracted. The obtained signals of thermal differences were smoothed using a 1-year gaussian filter to account for seasonal differences in phase shift and thermal amplitude in relation to the 5-year period, and the gaussian filters were subtracted from the initial thermal difference signals to obtain a high-frequency thermal residual signal that is related to advection events (Fig. 6). A multivariate correlation using the seasonal sinusoidal simulations and the obtained residual signals explains between 90 and 99% of the variance of the original CAT records except in two sites, LP4 and LP8, where 81 and 84% of the variance is explained respectively.

The most intense advection event occurred during the Filomena storm (January 2021). This storm brought exceptional amount of snow precipitation to central Spain and unusually cold weather persisted for almost a month. Fig. 6 illustrates that the advection event of Filomena occurred synchronously along different sites of the entrance corridor, with its thermal amplitude being attenuated away from the entrance corridor until the site LP5. Thus, the site LP6 and those sites located farther from the entrance do not record the advection event. Similar dynamics are obvious with other significant advection events that occurred during the 5-year period. Sites LP6 to LP8 record advection events, but they are not synchronous with the main advection events in the more external sites of the entrance corridor. The thermal anomalies recorded in these three sites, which are in the deeper section of the entrance corridor, have limited thermal amplitude (i.e., <0.6 °C), and their thermal anomalies are synchronous. Finally, the site LP9, located in the ample gallery beyond the entrance corridor does not record any thermal anomaly related to advection.

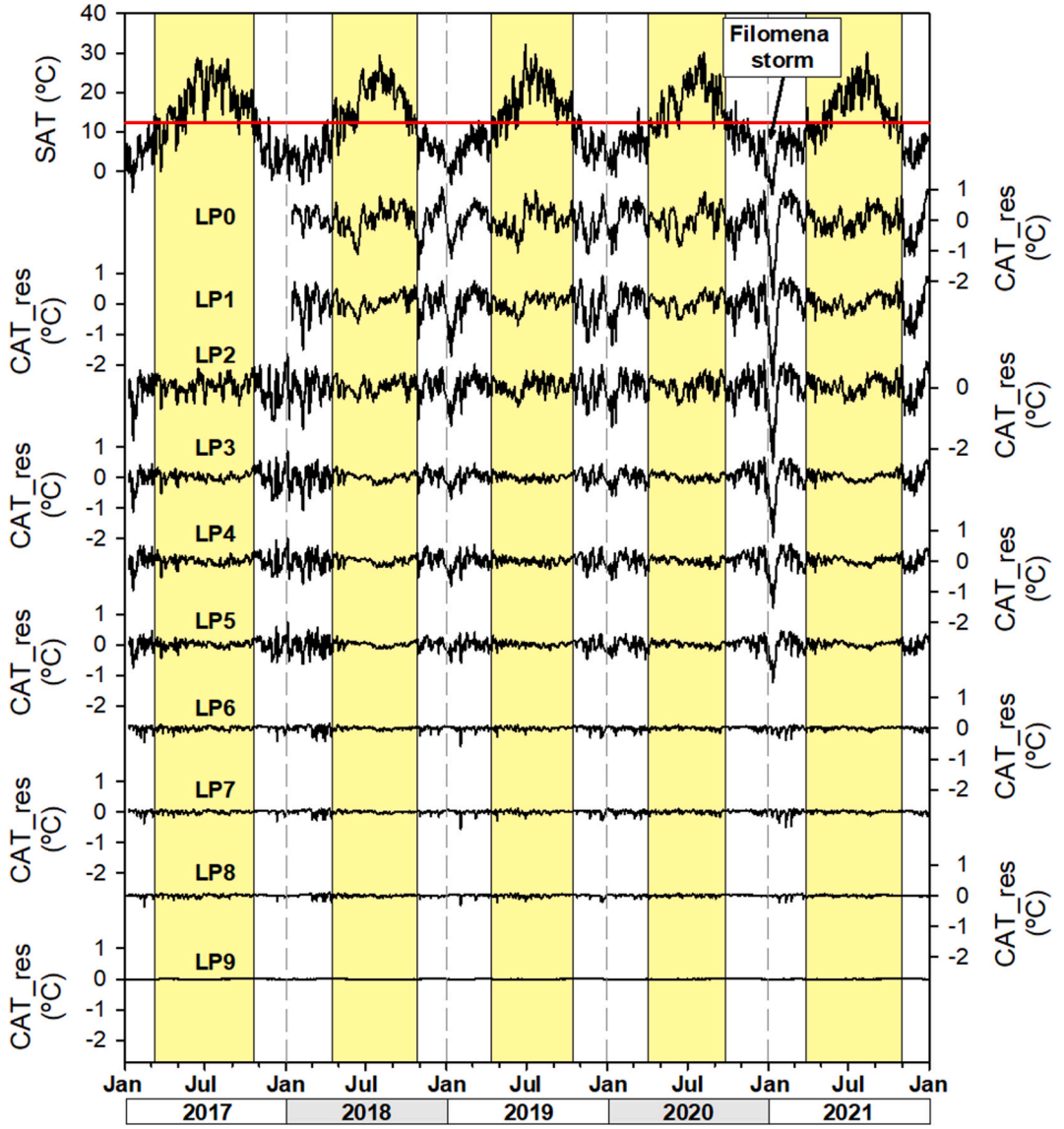

Fig. 6. Surface atmosphere temperature (SAT) compared to residual cave atmosphere temperature records (CAT_res). These cave records are expected to record thermal anomalies associated to advection events in the entrance of Los Pilones Cave. Notice that sites LP0 to LP5 record synchronous thermal anomalies such as the Filomena storm, which are not recorded in sites LP6 to LP8 that still record small thermal events, whereas the site LP9 does not record thermal anomalies related to advection events.

4. Discussion

4.1. Thermal conduction transferring SAT signals to caves

Pioneer studies of temperature in caves already identified thermal conduction as the main mechanism to transfer SAT to caves [14,15,18]. However, thermal advection has received more attention than conduction (e.g. Refs. [17,45–47]) since thermal anomalies related to advection are often associated to cave ventilation dynamics. Although in recent decades there have been significant advances in the knowledge of SAT transfer to caves or analogue environments by thermal conduction [9,24,32,34–36], most cave scientists ignore the implications that this mechanism has on CAT and thermal dependent proxies (e.g., thermal decoupling/asynchrony of SAT-CAT signals). The limited impact of advection in the thermal regime of Los Pilones Cave and the specific design of the experiment in this site to undoubtfully identify thermal conduction dynamics, results in a paradigmatic case that we hope will help cave scientists to understand the role of thermal conduction in controlling temperature of most caves.

To obtain the thermal diffusivity in Los Pilones Cave, the elevation of the ceiling was used to calculate bedrock thickness, because the average elevation of the gallery resulted in worst correlations of the phase shift and thermal amplitude with bedrock thickness. Although in an ideal system dominated by pure thermal conduction, half the height of the walls would have been the most logical choice, thermal transfer is slightly more complex. Our simulation does not include the role of radiation as a mechanism transferring the SAT signal, although radiation becomes important in transparent media (i.e., cave air). Cave walls and cave atmosphere exchange heat and although cave walls dominate the temperature of the cave atmosphere [15], modification of the cave atmosphere (e.g., by advection) also impacts the surficial temperature of cave walls [32]. In a 2-D simulation, Guerrier et al. [36] showed that radiation is responsible for muting thermal differences in the surface of cave walls in particular sections of rooms/galleries, and that the temperature of the cave walls approaches the temperature of the ceiling of the section considered, supporting the evidence found in our experimental analysis. So, in systems where advection has limited impact, there should be no major differences in the exact location of temperature

measurement, since for particular sections of galleries or rooms temperature tends to be homogenous due to radiation effects. So, by taking the height of the ceiling to calculate bedrock cover, we already accounted for the impact of radiation in the propagation of SAT signal to the cave.

Table 2 shows that the 1-D thermal conduction model explains >50% of the thermal variability observed in measured data from all sites. The model performs better in sites with the larger thermal anomalies related to thermal conduction or in sites with limited thermal impact of advection events. For those sites in the outer section of the entrance corridor, where advection events such as the one related to the Filomena storm are important (i.e., LP0 to LP5), there is a significant correlation (r^2 = 0.86, p-value<0.01) between the determination coefficient that correlates simulation and observational data (as shown in Table 2) and the ratio $Ln(A_z)/SD_{res}$ that represents the change in thermal variability of conduction versus advection in the studied sites. In this case, the natural logarithm of the simulated thermal amplitude captures thermal variability in a pure conduction system, whereas the standard deviation of residual thermal anomalies (series shown in Fig. 6), shows thermal variability associated to advection. The progressive reduction in thermal variability related to thermal conduction in sites with thicker bedrock cover is more efficient that the attenuation of thermal variability related to equilibration of air introduced by advection with the cave walls. This results in less thermal variability explained by the 1-D thermal conduction model in inner sites of the cave entrance corridor while advection still is important. On the other hand, in the inner section of the entrance corridor and in the cave interior beyond the entrance corridor, where advection events have a limited or negligible impact on thermal anomalies, the 1-D thermal conduction model explains >80% of the observed variability, confirming the key role of thermal conduction explaining CAT records even in sites with very limited thermal variability.

Thermal diffusivity in the entrance corridor of Los Pilones Cave during the period 2017–2021 was $5.07*10^{-7}$ $\pm1.27*10^{-7}$ m^2/s. This value is in the lower range of the thermal diffusivities reported in literature for carbonate rocks. Thermal diffusivity values measured in caves have been reported: $7.56*10^{-7}$ m^2/s [35], $8.0*10^{-7}$ m^2/s [36]. In their simulations Villar et al. [18] assumed a κ value of $11.0*10^{-7}$ m^2/s and Domínguez-Villar et al. [32] used a suit of possible κ values ranging from $5.2*10^{-7}$ m^2/s to $10.0*10^{-7}$ m^2/s where values between $7.0*10^{-7}$ m^2/s and $8.5*10^{-7}$ m^2/s were fitting better the observations. In their classical study, Carslaw and Jaeger [47], reported limestones having a κ value of $7.0*10^{-7}$ m^2/s, whereas in the extensive literature compilation of rocks thermal properties by Cermak and Rybach [11] carbonate rocks, including marbles, limestones, dolostones and marly carbonates (163 samples from 26 different localities) had values ranging from $3.1*10^{-7}$ m^2/s to $15.3*10^{-7}$ m^2/s being the average ± 2 SD of the 26 considered locations $9.73*10^{-7}$ $\pm3.36*10^{-7}$ m^2/s. Therefore, the value calculated in the entrance corridor of Los Pilones Cave is within the natural range of carbonate rocks, although it is biased towards lower diffusivity values of the distribution of reported thermal diffusivities. It should be noticed that our κ value was obtained experimentally from a karst massif and not from a carbonate rock in the laboratory. As a result of the relatively high solubility of carbonates, a karst massif is a heterogeneous media composed of three phases, rock, water and air. Thermal diffusivity of water in the range of environmental temperatures is around $1.44*10^{-7}$ m^2/s [48,49], whereas κ value of air is around $18.69*10^{-7}$ m^2/s [48,50]. So, an enhanced porosity of the rock with high degree of water content in its natural environment can justify the relatively low κ value. This scenario is consistent with the rock at the entrance of Los Pilones Cave that is a calcarenite composed of bioclasts that still preserve significant porosity after dolomitization.

The thermal diffusivity was calculated from the phase shift and thermal amplitude of the 5-year period. However, phase shift and thermal amplitudes were also calculated for six-month periods (n = 9), and their variability was used to calculate the uncertainty of the thermal diffusivity. Differences in the seasonal phase shifts in comparison with the 5-year period are on average < 7 days, although advection events make particular seasons having significant shifts in the cross-correlation analysis (up to 40 days in the season that accounts for Filomena storm). On the other hand, thermal amplitudes show variations (2 SD) representing 12–53% of the 5-year average thermal amplitude depending on the site. These data show that the empirical calculation of thermal diffusivity has certain variability through time. Variability within one site cannot be attributed to rock heterogeneity, since changes in porosity are expected to be negligible during the 5-year period studied. However, the amount of water in the matrix porosity of the rock might change through time [51–53]. Since residence time of water flowing through matrix porosity is often >1 year even in shallow caves (e.g. Refs. [54–56]), seasonality of precipitation is not expected to dominate water content variability of the karst massif, although the ratio of water in the matrix porosity changes through time potentially having certain impact on the thermal diffusivity. The reported uncertainty of the calculated thermal diffusivity in Los Pilones Cave represents ±23% of thermal diffusivity which includes, among other sources of uncertainty affecting the κ value, the variability of the water in the rock massif.

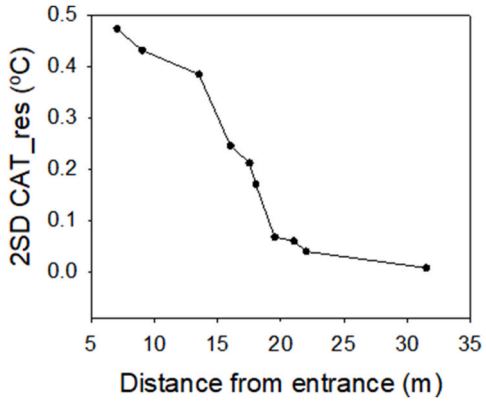

Fig. 7. Graph comparing the magnitude of thermal anomalies associated to advection, reported as the 2 SD of the records of residual cave atmosphere temperature (CAT_res), with the distance to the cave entrance. The larger thermal anomalies associated to advection are recorded in sites closer to the entrance, where interaction of the intruding air and cave walls still is limited. Major changes in the slope of this graph are related to significant topographical constraints in the cave entrance or changes in the cave airflow dynamics.

4.2. Advection in the entrance corridor of Los Pilones Cave

The larger thermal anomalies in caves are typically recorded in their entrances due to intrusion of external air by advection [25]. As expected, the entrance of Los Pilones Cave records thermal anomalies associated to advection (Fig. 6), although in this case, even in the entrance, conduction dominates the thermal variability (i.e., conduction model already explains >50% of the variance of all studied sites). This is the result of the constrained entrance of this cave that limits the advection of external air into its entrance corridor. At daily scale, the advection events should occur synchronously along the entrance corridor of the cave and the thermal amplitude of the anomalies decrease with distance to the entrance due to the attenuation impact of the cave walls. The thermal variability of the signal associated to advection decreases with the distance to the cave entrance confirming the expectations (Fig. 7). However, when thermal anomalies associated to advection are compared between contiguous sites (e.g., LP1 and LP2), determination coefficients (r^2) are >0.85 for all paired sites with two exceptions LP5-LP6 and LP8-LP9. Thus, three sections of the cave can be identified: the most external sector of the cave entrance (including sites LP0 to LP5), the internal sector of the cave entrance (including sites LP6 to LP8) and the inner galleries of the cave (site LP9 being representative of the thermal

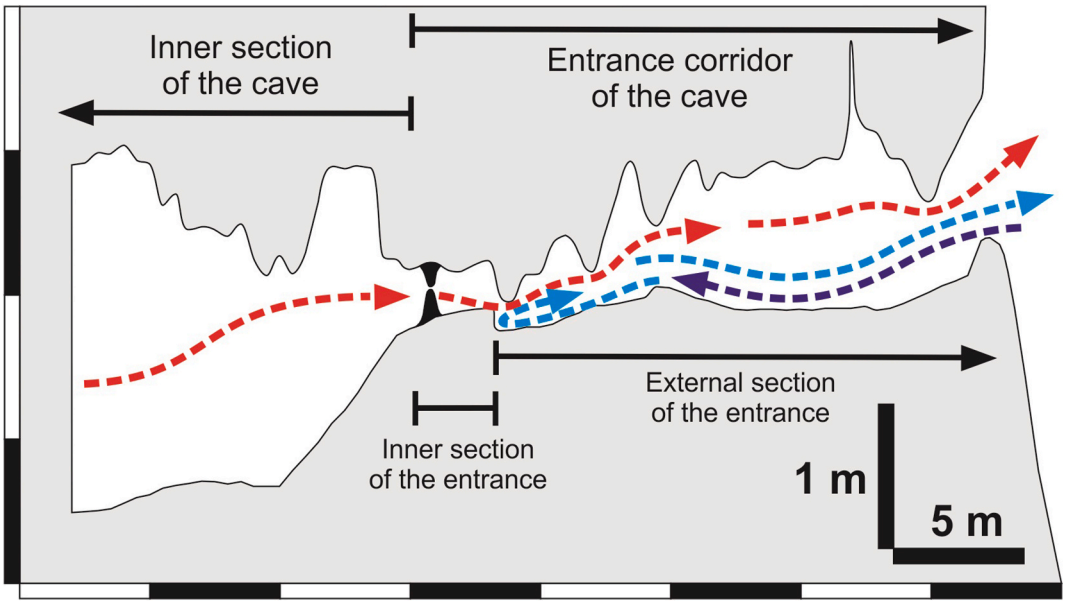

Fig. 8. Cave profile sketch showing the airflow dynamics in the entrance sector of Los Pilones Cave. The inner section of Los Pilones Cave is ventilated by a subtle outflow of air all year round that does not cause thermal anomalies, since the temperature of air entering the cave is already equilibrated with the bedrock. In the inner section of the entrance corridor, limited thermal anomalies occur during events of enhanced outflow ventilation due to the Venturi effect, forced by the constrained morphology of the passages. The external section of the cave entrance corridor often records events of intrusions of external air into the cave, with an impact limited to the section not constrained by significant topographical barriers.

anomalies associated to advection recorded in the rest of the cave). Large advection events such as the one that occurred during Filomena storm are limited to the section that includes the more external sites. The corridor has the lower ceiling elevation between sites LP5 and LP6 and in addition, a step elevates the ground around 0.1 m right after this constraint. These topographic barriers coincide with a change in the azimuth of the cave which results in advection events of external air not entering beyond this point of the cave (Fig. 8). However, the internal section of the corridor entrance of the cave still records small advection events. These events occur occasionally during the winter season and can only be the result of cave air outflow. In fact, they can be identified even in the more external section of the entrance corridor, although they are less obvious due to their smaller thermal amplitude. The inner section of the cave does not record thermal anomalies related to advection, although this does not mean that advection does not take place. Spot measurements of cave air CO_2 supports that the cave is well ventilated during all seasons. Thus, the lack of thermal anomalies related to advection suggests that the inflow of air to the cave interior originates from atmospheres already equilibrated with bedrock temperature. Although the dynamics of Los Pilones Cave ventilation still is under investigation, the most likely cause of the outflow of air through the cave is a barometric gradient that causes a permanent flow of air from the karst underneath the cave to the exterior, using the cave galleries as preferential conduits to facilitate the outflow. Despite thermal anomalies associated to advection are not recorded in the ample sections of the cave interior, the morphological constrain that represents the entrance corridor of the cave has to force slight drops in pressure due to the Venturi effect. These occasional drops in atmospheric pressure, caused by the outflow of air through a constraint section of the cave, are expected to occur during events of enhanced outflow and, according to the gasses law, will result in proportional drops of temperature, explaining the small drops of temperature that are more obviously recorded in the inner section of the entrance corridor. A sketch of the ventilation dynamics in the cave entrance is shown in Fig. 8.

5. Conclusion

Temperature was recorded in the entrance sector of Los Pilones Cave and above the cave during five years. The transfer of SAT signal to the cave is dominated by thermal conduction as confirmed by a 1-D model. Thermal conduction caused seasonal oscillations to be attenuated with increasing thickness of bedrock cover and thermal signals were transmitted to the cave with certain delay that also depended on the thickness of bedrock cover. In the studied case, less than 15 m of rock overburden caused half year of delay in the thermal signal resulting in thermal decoupling between SAT ad CAT. The thermal diffusion coefficient in the entrance corridor of Los Pilones Cave during the period 2017–2021 was $5.07*10^{-7} \pm 1.27*10^{-7}$ m^2/s. Since karst is composed of rock water and air, we speculate that changes in the measured thermal diffusivity, accounted in its uncertainty, are in part related to changes in the ratio of water/air in rock porosity through time. Los Pilones Cave is a paradigmatic case in which seasonal ventilation has a limited impact on temperature records that are instead mainly controlled by thermal conduction even in the entrance sector of the cave. Thermal conduction is thought to dominate thermal signals in the inner sections of most caves, with seasonal advection having secondary roles that introduce variable and transitory thermal anomalies. Thus, we expect that this research will serve as a paradigmatic example to show how thermal conduction operates in caves and the important implications that this signal transfer has in the underground environment (e.g., thermal decoupling).

Declaration of competing interest

The authors declare that they have no known competing financial interests or personal relationships that could have appeared to influence the work reported in this paper.

Data availability

Data will be available after publication in the open repository Gredos at https://gredos.usal.es

Acknowledgements

The project leading to this research has received funding from the European union's Horizon 2020 research and innovation programme under the Marie Skłodowska-Curie grant agreement No. 101030314. We would like to thank the assistance during fieldtrips to Ramón Martín Ocaña, Lucía Gómez Ruiz and Juan Montero Martín and to all speleologists that respected this scientific experiment. We also appreciate the support of Máximo Manrique García who gave permission to access and perform research in this cave.

References

[1] J.H. Davies, Global map of solid Earth surface heat flow, G-cubed 14 (2013) 4608–4622.
[2] M. B Stevens, J.F. González-Rouco, H. Beltrami, North America climate of the last Millennium: underground temperatures and model comparison, Journal of geophysical research-earth surface 113 (2008), F01008.
[3] H.N. Pollack, S. Huang, Climate reconstruction from subsurface temperatures, Annu. Rev. Earth Planet Sci. 28 (2000) 339–365.
[4] H. Beltrami, Surface heat flux histories from inversion of geothermal data: energy balance at the Earth's surface, J. Geophys. Res. Solid Earth 106 (B10) (2001) 21979–21993.
[5] M.P. Anderson, Heat as a groundwater tracer, Ground Water 43 (2005) 951–968.
[6] K. Labs, Regional-analysis of ground and above-ground climate, Undergr. Space 7 (1982) 37–65.
[7] W.A. Jury, R. Horton, Soil Physics, Wiley, New York, 2004.
[8] H.N. Pollack, J.E. Smerdon, P.E. van Keken, Variable seasonal coupling between air and ground temperatures: a simple representation in terms of subsurface thermal diffusivity, Geophys. Res. Lett. 32 (2005), L15405.
[9] G.C. Rau, M.O. Cuthbert, M.S. Andersen, A. Baker, H. Rutlidge, M. Markowska, H. Roshan, C.E. Marjo, P.W. Graham, R.I. Acworth, Controls on cave drip water temperature and implications for speleothem-based paleoclimate reconstructions, Quat. Sci. Rev. 127 (2015) 19–36.
[10] D. Domínguez-Villar, K. Krklec, J.A. López-Sáez, F.J. Sierro, Thermal impact of Heinrich stadials in cave temperature and speleothem oxygen isotope records, Quat. Res. 101 (2021) 37–50.
[11] V. Cermak, L. Rybach, Thermal conductivity and specific heat of mineral sand rocks, in: G. Angenheister (Ed.), Landolt-Börnstein: Zahlenwerte und Funktionen aus Naturwissenschafen und Technik, Springer-Verlag, Berlin, 1982, pp. 305–343.
[12] D. Ford, P. Williams, Karst Hydrology and Geomorphology, John Wiley & Sons Ltd, Chichester, 2007.
[13] G.W. Moore, Cave temperature, NSS (Natl. Speleol. Soc.) News 22 (1964) 57–60.
[14] G.W. Moore, G. Nicholas, Out of Phase Seasonal Temperature Fluctuations in Cathedral Cave, Kentucky, vol. 76, Geological Society of America Special Paper, 1964, p. 313.
[15] J.B. Cropley, Influence of surface conditions on temperatures in large cave systems, Bull. Natl. Speleol. Soc. 27 (1) (1965) 1–10.
[16] A. Pflitsch, J. Piasecki, Detection of an airflow system in niedzwiedzia (bear) cave, kletno, Poland, J. cave and karst stud. National Speleological Soc. Bulletin 65 (3) (2003) 160–173.
[17] T.M.L. Wigley, M.C. Brown, The physics of caves, in: T.D. Ford, C.H.D. Cullingford (Eds.), The Science of Speleology, Academic Press, London, 1976, pp. 329–358.
[18] E. Villar, P.L. Fernández, L.S. Quindos, J.R. Solana, J. Soto, Temperature of rock surfaces in altamira cave (Spain), Trans. Br. Cave Res. Assoc. 10 (1983) 165–170.
[19] G.W. Moore, G.N. Sullivan, Speleology: the Study of Caves, Zephyrus Press, Teaneck NJ, 1978.
[20] A. Bögli, Karst Hydrology and Physical Speleolology, Springer Verlag, Berlin, 1980.
[21] G. Badino, Física del Clima Sotterraneo. vol. 7 Serie II, Memoria dell'Instituto Italiano di Speleologia, Bologna, 1995.
[22] G. Badino, Underground drainages systems and geothermal flux, Acta Carsol. 34 (2005) 277–316.
[23] M. Luetscher, P.Y. Jeannin, Temperature distribution in karst systems: the role of air and water fluxes, Terra. Nova 16 (2004) 344–350.
[24] M. Luetscher, B. Lismonde, P.Y. Jeannin, Heat exchanges in the heterometric zone of a karst system: monlesi cave, Swiss Jura Mountains, J. Geophys. Res. 113 (2008), F02025.
[25] P.A. Smithson, Inter-relationships between cave and outside air temperatures, Theor. Appl. Climatol. 44 (1991) 65–73.
[26] J. Faimon, D. Troppová, V. Baldíkm, R. Novotný, Air circulation and its impact on microclimatic variables in the císařská cave (morovian karst, Czech republic), Int. J. Climatol. 32 (2011) 599–623.
[27] A.N. Palmer, Cave Geology, Cave Books, Dayton (OH), 2007.
[28] C. Spötl, I.J. Fairchild, A. Tooth, Cave air on drip water geochemistry, Obir caves (Australia): implications for speleothem deposition in dynamically ventilated caves, Geochem. Cosmochim. Acta 69 (2005) 2451–2468.
[29] A. Pflitsch, M. Wiles, R. Horrocks, J. Piasecki, J. Ringeis, Dynamic climatologic processes of barometric cave systems using the example of Jewel Cave and Wind Cave in South Dakota, USA, Acta Carsol. 39 (2010) 449–462.
[30] F. Bourges, P. Genthon, A. Mangin, D. D'Hulst, Microclimates of L'aven D'orgnac and other French limestone caves (chaveaut, esparros, marsoulas), Int. J. Climatol. 26 (2006) 1651–1670.
[31] M.O. Cuthbert, G.C. Rau, M.S. Andersen, H. Roshan, H. Rutlidge, C.E. Marjo, M. Markowska, C.N. Jex, P.W. Graham, G. Mariethoz, R.I. Acworth, A. Baker, Evaporative cooling on speleothem drip water, Sci. Rep. 4 (2014) 5162.
[32] D. Domínguez-Villar, S. Lojen, K. Krklec, A. Baker, I.J. Fairchild, Is global warming affecting cave temperatures? Experimental and model data from a paradigmatic case study, Clim. Dynam. 54 (2015) 569–581.
[33] D. Domínguez-Villar, Heat flux, in: I.J. Fairchild, A. Baker (Eds.), Speleothem Science. From Processes to Past Environments, Wiley-Blackwell, Chichester, 2012, pp. 137–145.
[34] F. Perrier, J.L. Le Mouël, J.P. Poirier, M.G. Shnirman, Int. J. Climatol. 25 (2005) 1619–1631.
[35] D. Domínguez-Villar, I.J. Fairchild, A. Baker, R.M. Carrasco, J. Pedraza, Reconstruction of cave temperature based on surface atmosphere temperature and vegetation changes: implications of speleothem palaeoclimate records, Earth Planet Sci. Lett. 369–370 (2013) 158–168.
[36] B. Guerrier, F. Doumenc, A. Roux, S. Mergui, P.Y. Jeannin, Climatology in shallow caves with negligible ventilation: heat and mass transfer, Int. J. Therm. Sci. 146 (2019), 106066.
[37] M. Fernández Tabera, Avances a los catálogos de cavidades de las provincias de Madrid y Segovia, Federación Madrileña de Espeleología, Madrid, 1979.
[38] A. Alonso, El Cretácico de la Provincia de Segovia (borde Norte del Sistema Central), vol. 7, Seminarios de Estratigrafía, Madrid, 1981, p. 271. UCM-CSIC.
[39] W. Köppen, R. Geiger, Das geographische System der Klimate, 1936. Berlin.
[40] D.A. Nafría García, N. Garrido del Pozo, M.V. Álvarez Arias, D. Cubero Jiménez, M. Fernández Sánchez, Villarino, I. Barrera, A. Gutiérrez García, I. Abia Llera, Atlas Agroclimático de Castilla y León. ITACYL-AEMET, 2013. http://atlas.itacyl.es.
[41] B. Heeb, Proceedings of the IV European Speleological Congress, in: Paperless Caving – an Electronic Cave Surveying System, French Federation of Speleology, Vercors, 2008, pp. 130–133.
[42] E. David, Visual Topo V. 5.11, Spéléo Club de la Seine, 2019. http://vtopo.free.fr.
[43] J.E. Smerdon, H.N. Pollack, J.W. Enz, M.J. Lewis, Conduction-dominated heat transport of the annual temperature signal in soil, J. Geophys. Res. 108 (B9) (2003) 2431.
[44] J. Bodzenta, B. Burak, M. Nowak, M. Pyka, m. Szałajko, M. Tanasiewicz, Measurement of the thermal diffusivity of dental filling materials using modified Ångström method, Dent. Mater. 22 (2006) 617–621.
[45] T.C. Atkinson, P.L. Smart, T.M.L. Wigley, Climate and natural radon levels in castleguard cave, columbia icefields, alberta, Canada, Arct. Alp. Res. 15 (4) (1983) 487–502.
[46] C.R. de Freitas, R.N. Littlejohn, Cave climate: assessment of heat and moisture exchange, J. Climatol. 7 (1987) 553–569.
[47] M.D. Covington, A.J. Luhmann, F. Grabrovšek, M.O. Saar, C.M. Wicks, Mechanisms of heat exchange between water and rock in karst conduits, Water Resour. Res. 47 (2011), W10514.
[48] H.S. Carslaw, J.C. Jaeger, Conduction of Heat in Solids, second ed., Oxford University Press, New York, 1959.
[49] D.W. James, The thermal diffusivity of ice and water between -40 and +60 °C, J. Mater. Sci. 3 (1968) 540–543.
[50] W.J. Massman, Molecular diffusivities of Hg vapor in air, O_2 and N_2 near STP and the kinematic viscosity and thermal diffusivity of air near STP, Atmos. Environ. 33 (1999) 453–457.
[51] C. Bradley, A. Baker, C.N. Jex, M.J. Leng, Hydrological uncertainties in the modelling of cave drip-water d^{18}O and the implications for stalagmite paleoclimate reconstructions, Quat. Sci. Rev. 290 (2010) 2201–2214.
[52] J.W. Moerman, K.M. Cobb, J.W. Partin, A.N. Meckler, S.A. Carolin, J.F. Adkins, S. Lejau, J. Malang, B. Clark, A.A. Tuen, Transformation of ENSO-related rainwater to dripwater $\delta^{18}O$ variability by vadose water mixing, Geophys. Res. Lett. 41 (2014) 7907–7915.
[53] D. Domínguez-Villar, S. Lojen, K. Krklec, R. Kozdon, R.L. Edwards, H. Cheng, Ion microprobe $\delta^{18}O$ analyses to calibrate slow growth rate speleothem records with regional $\delta^{18}O$ records of precipitation, Earth Planet Sci. Lett. 482 (2018) 367–376.
[54] J.B. Chapman, N.L. Ingraham, J.W. Hess, Isotopic investigation of infiltration and unsaturated zone flow processes at Carlsbad Cavern, New Mexico, J. Hydrol. 133 (1992) 343–363.
[55] D. Domínguez-Villar, K. Krklec, I. Boomer, I.J. Fairchild, ISODRIP, a model to transfer the δ18O signal of precipitation to drip water — implementation of the model for Eagle Cave (central Spain), Sci. Total Environ. 797 (25) (2021), 149188.
[56] T. Kluge, D.F.C. Riechelmann, M. Wieser, C. Spötl, J. Sültenfuß, A. Schröder-Ritzrau, S. Niggemann, W. Aeschbach-Hertig, Dating cave drip water by tritium, J. Hydrol. 394 (2010) 396–406.